Food Chemistry: X 23 (2024) 101748

Contents lists available at ScienceDirect

Food Chemistry: X

journal homepage: www.sciencedirect.com/journal/food-chemistry-x

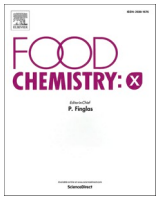

Stabilization of fermented tomato (*Solanum lycopersicum* L.) juice by differently charged hydrocolloids

Lei Zhao [a,1], Yu Wang [a,1], Ruxianguli Maimaitiyiming [a], Runhan Liu [a], Liang Wang [a], Ruoqing Liu [a], Keping Chen [b], Aihemaitijiang Aihaiti [a,*], Jingyang Hong [a,*]

[a] *School of Life Science and Technology, Xinjiang University, Urumqi 830000, China*
[b] *Xinjiang Huize Food Limited Liability Company, Urumqi 830000, China*

ARTICLE INFO

Keywords:
Fermented tomato (*Solanum lycopersicum* L.) juice
Soluble soybean polysaccharide
Chitosan
Pullulan polysaccharide
Stability

ABSTRACT

This study investigated the impact of three different charged hydrocolloids, anionic polysaccharide (soluble soybean polysaccharide, SSPS), neutral polysaccharide (pullulan polysaccharide, PUL), and cationic polysaccharide (chitosan, CS), and their complexation on the stabilization efficiency of fermented tomato juice (FTJ). The effect of hydrocolloids on FTJ under different treatment conditions were comprehensively evaluated by determining the particle size distribution, zeta potential, rheological properties, Fourier transform infrared spectroscopy, surface tension, and LUMiSizer. The combined conditions suggest that PUL exhibits better storage stability than SSPS and CS when used individually. Compared with the use of the stabilizers, the combination of hydrocolloids had a greater impact on the storage stability of the FTJ, and the storage stability of the FTJ increased when 0.15% SSPS + 0.03% PUL + 0.15% CS was added. This study lays the groundwork for the development of stable fruit juice beverages.

1. Introduction

The tomato (*Solanum lycopersicum* L.) is among the most widely recognized vegetables globally and is renowned for its rich array of nutrients, including lycopene, vitamins, organic acids and various other beneficial compounds (Giovanelli & Paradiso, 2022). In 2020, global tomato production surpassed 1.86 billion tons (FAO, 2020, https://www.fao.org/faostat/en/ - data/QCL, accessed April 25, 2022). Tomato-based beverages, are popular drinks because of their natural nutritional content and delightful taste worldwide. Fredrik et al. (2020) studies have highlighted the significant value of tomato beverages, citing their antioxidant, anti-inflammatory, and potentially anticancer properties, which contribute to their widespread consumer appeal. However, tomato beverages are prone to sediment formation, particularly in homemade or inadequately processed varieties, potentially stemming from residual pulp or other insoluble substances. This sediment can adversely impact beverages' taste and overall quality. Therefore, addressing the sediment in bottled beverages, which is considered a quality defect. Measures to enhance the dispersion of suspended particles are essential for ensuring product consistency and stability.

The particle size of fruit juices is a critical factor for the stability of cloudy beverages (Tiwari et al., 2009). Compared with larger particles, smaller particles create a more stable suspension and are less prone to settling during storage. Stokes's law elucidates this phenomenon by describing the settling velocity of particles in a fluid, taking into account variables such as particle diameter, density, fluid viscosity, and gravity (Lisa et al., 2023). Research has demonstrated that high-pressure homogenization can markedly decrease the particle size in tomato juice, thereby enhancing the stability and managing sedimentation (Pedro et al., 2013). Furthermore, the hydrocavitation (HC) technique has been shown to bolster the stability of tomato juice by generating cavitation effects, which lead to a reduction in particle size and an increase in apparent viscosity, ultimately contributing to greater stability (Ruly et al., 2019). Despite the efficacy of these techniques, their adoption in industry is somewhat constrained by the high capital and operational costs involved.

There are few studies on the use of hydrocolloids to enhance the stability of tomato juice. Hydrocolloid is a polysaccharide commonly used in the food, health, and cosmetic industries because of its ability to change the rheological properties of foods and improve their stability,

* Corresponding authors.
E-mail addresses: 2386935884@qq.com (A. Aihaiti), hongjingyang2017@126.com (J. Hong).
[1] Lei Zhao is the first author of this paper and Yu Wang is the co-first author of this paper.

https://doi.org/10.1016/j.fochx.2024.101748
Received 21 June 2024; Received in revised form 11 August 2024; Accepted 16 August 2024
Available online 20 August 2024

fluidity, and texture (Sinchaipanit et al., 2013). The incorporation of hydrocolloids with different charge properties into the juice can result in diverse effects on the juice's stability and potential mechanisms for stabilization efficiency.

Soluble soy polysaccharide is an anionic polysaccharide obtained from soy protein byproducts. It is characterized by high water solubility and low viscosity as a stabilizer (Yoo et al., 2006). SSPS possesses a compact, highly branched spherical structure with a short main chain and long side chains. The main chain consists of alternating units of galacturonic acid and rhamnogalacturonic acid, with galacturonic acid formed from D-galacturonic acid (D-GalA) linked through α-1,4 glycosidic bonds. Poly-rhamnogalacturonic acid features alternating D-GalA and L-rhamnose linkages. The uncharged side chains contain galactose, arabinose, and galacturonic acid, along with trace amounts of fucose, xylose, and glucose.Owing to their distinctive main and side chain structures, soluble soy polysaccharides exhibit lower viscosity and improved stability in beverages than high methoxyl pectin and guar gum (Nakamura et al., 2006). Furthermore, the negatively charged soluble soy polysaccharide can interact with the positively charged chitosan (CS). CS is a linear polymeric carbohydrate derived from the deacetylation of the C2 amino group in chitin (No & Prinyawiwatkul, 2009). The chemical structure of CS was illustrated in Fig. 1A and Fig. 1B (Okuyama et al., 2000). When the degree of deacetylation exceeds 50%, chitosan typically dissolves in an acidic environment, where it transforms into a cationic polyelectrolyte and an alkaline polysaccharide.

Its polyelectrolyte properties, polysaccharide properties, electrostatic binding properties, and viscosity characteristics can enhance food stability, prevent layering or precipitation in juice beverages, extend the shelf life of food, enhance the nutritional value of food, promote human health, and make it an ideal stabilizer (Hartgerink et al., 2001). Pullulan polysaccharide (PUL) is an extracellular polysaccharide produced by Aureobasidium pullulans. PUL is composed of glucose units linked by α-1,4-glycosidic bonds to form maltotriose. These maltotriose units are further polymerized via α-1,6-glycosidic bonds, resulting in a linear polysaccharide with a stepped, rod-like structure, as shown in Fig. 1C (Xiao et al., 2017). This linear arrangement endows pullulan with excellent film-forming properties and enzymatic degradation capabilities (Shingle et al., 2004). PUL is soluble in water, with a neutral solution that does not easily precipitate or crystallize but easily coagulates into a gel. The viscosity of a PUL solution is influenced by molecular weight and not by heat, pH, or most metal ions (Ram et al., 2019).

Currently, there is no available information regarding the use of the three mentioned hydrocolloids in fermented tomato juice (FTJ). It is unclear which parameters maintain turbidity stability, and this has not been systematically documented. Furthermore, the simultaneous use of the three hydrocolloids has not been examined in other juices, although chitosan was incorporated into collagen peptide cranberry juice for stabilization and antimicrobial effects (Zhang et al., 2023).

This study aimed to examine the influence of three water colloids SSPS, PUL, and CS each with different charges, on the zeta potential, particle size, rheological properties, Fourier transform infrared (FTIR) spectroscopy, and surface tension of FTJ. The goal of this study was to investigate the effects of individual stabilizers and their combinations on the stability of FTJ. Additionally, the stability of LUMiSizer was further assessed. LUMiSizer analysis method is a recent advancement in stability testing for liquid fruit and vegetable juices, emulsions, and other products. This method utilizes Lambert-Beer's law, Stokes' law, and centrifugal acceleration techniques to evaluate product stability, thereby reducing testing time and increasing research efficiency It uses Lambert-Beer's law, Stokes' law, and centrifugal acceleration techniques to evaluate product stability, reducing testing time and improving research efficiency (Dammak et al., 2018).

2. Materials and methods

2.1. Materials

Tomato paste was obtained from Xinjiang Huize Food Limited Liability Company. (Xinjiang, China). FTJ was obtained from Xinjiang University (Xinjiang, China). *Lactobacillus fermentum (L. fermentum)* Center of Industrial Culture Collection (CICC) 21,800, *Lactobacillus plantarum (L. plantarum)* CICC 21797, *Lactobacillus casei (L. casei)* CICC 6114, and *Pediococcus pentosaceus (P. pentosaceus)* CICC 21862 were obtained from the China CICC (Beijing, China). SSPS was obtained from Shandong Juyuan Biotechnology Co., Ltd. (Shandong, China). PUL was acquired from Henan Wanbang Chemical Technology Co., Ltd. (Henan, China), and CS was purchased from Shanghai Yuanye Biotechnology Co., Ltd. (Shanghai, China). MRS broth medium was purchased from Guangdong Hankai Microbial Technology Co.

2.2. Sample preparation

FTJ was prepared following the previous research conducted by our group Zhao and Hong (2024). Initially, tomato paste was diluted with water and mixed thoroughly in a ratio of 1:2.6 to create tomato juice. Fermentation was then initiated to prepare FTJ. The TSS was adjusted to 12.5°Brix and then sterilized at 90 °C for 10 min. Pectinase at 1.5% (*w/v*), cellulase at 1% (w/v), and hemicellulase at 1% (w/v) were added to the samples and enzymatically digested at 57 °C for 3 h. The samples were sterilized at 90 °C for 30 min. The total bacterial density in FTJ was 3×10^6 CFU/mL. *P. pentosaceus, L. casei, L. plantarum,* and L. *fermentum* were mixed in the ratio of 53.79%, 13.17%, 19.87%, and 13.17%. Finally, fermentation was conducted for 22 h in a constant temperature oscillation incubator (model ZD-85 A, Changzhou, China, set at 37 °C).

2.3. Zeta potential measurement

A sample was dispersed in deionized water at a concentration of 0.01% by mass and sonicated for 3 min, after which the zeta potential was measured using a Malvern Instruments nanoparticle size analyzer

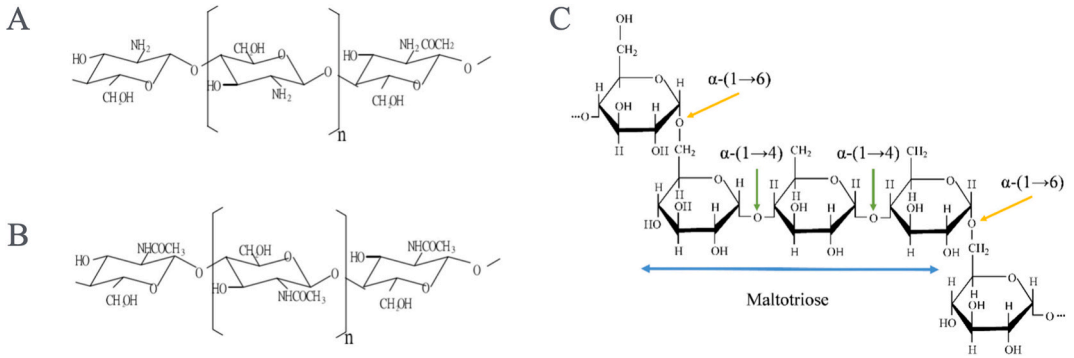

Fig. 1. A: Chemical structure formula of Chitosan; B: Chemical structure formula of chitin; C: Chemical structure formula of pullulan polysaccharide.

(Malvern Mastersizer ZS-90, UK) (Niu et al., 2022).

2.4. Particle size distribution (PSD)

The PSD of the samples was determined by a laser particle size distribution analyzer (Malvern Mastersizer 2000, UK). One milliliter of sample was taken from each of the experimental and control groups described above, diluted 10-fold with water, and then measured after thorough mixing. In addition, the volume-based mean diameter (D[4,3]) and the area-based mean particle size (D[3,2]) were calculated using the software provided by the device(Dai et al., 2019).

2.5. Measurement of rheological properties

Rheological property analysis was carried out at a temperature of 20 °C using a rotational rheometer with parallel plate geometry (60 mm in diameter) from Anton Paar (Model MCR92, Austria). The sample was deposited onto the base plate. The gap between the parallel plates was set at 0.5 mm, and the sample was allowed to equilibrate for one minute at 20 °C before measurements were taken. The shear rate applied ranged from 0.001 to 1000 s^{-1} (Lisa et al., 2023).

2.6. FTIR

The method described by Paola et al. (2024), with minor modifications. All samples were dried and then mixed with potassium bromide powder by grinding (1 mg sample/50 mg potassium bromide) to prepare the precipitate. The potassium bromide powder was dried at approximately 100 °C for 24 h. The grinding process needed to be performed under infrared light to minimize water errors. The samples were scanned 64 times at a resolution of 4 cm^{-1} in the range of 4000–450 cm^{-1} using an FTIR spectrometer (PerkinElmer, Waltham, MA, USA). The spectra of the samples were preprocessed using spectroscopy software, including the removal of background interferences, baseline correction, and normalization.

2.7. Surface tension test

The parameters of the instrument were set (Dataphysics DCAT21, Germany), and the platform with 20 mL of liquid was allowed to rise continuously and stop when it touched the platinum plate. After the platform clicks, the platinum plate contact liquid continues to rise due to the decrease in the buoyancy effect of the balance, which decreases to the set value after the instrument defaults the detection of the liquid level and storage platform position. The platform continues to rise to the set depth of immersion (generally 5 mm), the platform moves down to the stored position, the instrument begins to measure, and the test value that reaches the set stop conditions automatically stops.

2.8. Long-term stability measurements

A 425 μL sample was pipetted into a test tube (2 mm × 8 mm), filled with the sample, and then placed sequentially into the LUMiSizer (LUMiSizer651, Germany) machine. The sample was scanned and analyzed by a near-infrared beam at a wavelength of 865 nm. The scanning parameters were set to 1× the scanning light intensity, 25 °C, and 4000 r/min for one hour at 30 s intervals for a total of 120 scans to determine the radial position as a function of time. At the end of the scanning, the corresponding spatial-temporal extinction pattern, integrated transmittance, and sedimentation rate of the samples were analyzed by SEPView6, the analysis software accompanying the full-featured stability analyzer.

2.9. Statistical analysis

Data are expressed as the mean plus or minus standard deviation. Analysis of variance and Duncan's multiple range tests were performed using SPSS 26.0 (SPSS Science, Chicago, USA). Statistical significance ($P < 0.05$; Duncan test) Plotting was performed using Origin 2023 (OriginLb, Northampton, MA).

3. Results and discussion

3.1. PSD and zeta potential

A higher absolute value of the zeta potential indicates greater stability of the system, corresponding to strong electrostatic repulsion and reduced particle aggregation (Wei et al., 2020). Hydrocolloids can enhance electrostatic repulsion at the interface of the juice drink while contributing to the adsorption of a protective layer (Liu et al., 2016). As depicted in Fig. 2, the absolute value of the zeta potential of the samples is greater than that of the control when either a single hydrocolloid sample or a combination of hydrocolloid samples is added, indicating that the zeta potential of the samples is influenced by the concentration and type of hydrocolloid.

SSPS is an anionic polysaccharide, and the addition of different concentrations of SSPS to FTJ results in varying degrees of increase in the absolute value of the zeta potential, indicating different strengths of electrostatic interactions on the surface (Souza et al., 2012). The absolute value of the zeta potential decreased as the concentration of SSPS gradually increased, which could be attributed to the decrease in the surface charge of the molecules, leading to a decrease in electrostatic repulsion between the molecules and promoting their aggregation. In summary, the incorporation of SSPS suggested that the electrostatic interactions between the negatively charged hydrocolloids and the juice particles in the samples affect the stability of the FTJ. PUL is a neutral polysaccharide, and despite its neutrality, its addition significantly enhanced the absolute value of the zeta potential of the samples, indicating that the negative zeta potential of the FTJ was caused by the negative charge of the particles in the FTJ. Consistent with previous findings, the zeta potential of β-glucan (a neutral polysaccharide) added to collagen peptide solutions was greater than that of collagen peptide solutions without added β-glucan (Huang et al., 2021). CS is a cationic polysaccharide, and the zeta potential of FTJ was not significantly increased by CS, possibly because the negatively charged groups in FTJ neutralized some of the positive charges of CS. This slight increase may be due to the exposure of some positively charged groups, and the

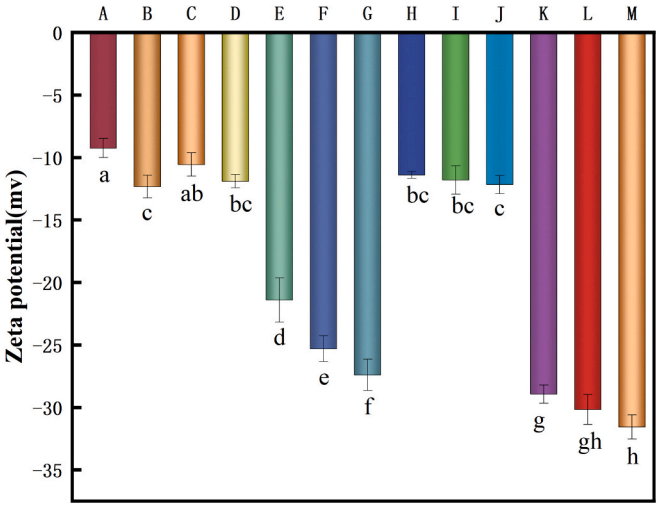

Fig. 2. Zeta of FTJ treated with different hydrocolloids. A: Blank; B: 0.15% SSPS; C: 0.2%SSPS; D: 0.25%SSPS; E: 0.02%PUL; F: 0.04%PUL; G: 0.06%PUL; H: 0.2%CS; I: 0.25%CS; J: 0.3%CS; K: 0.05%SSPS+0.01%PUL + 0.05%CS; L: 0.1%SSPS+0.02%PUL + 0.1%CS; M: 0.15%SSPS+0.03%PUL + 0.15%CS. Different lowercase letters indicate significant differences.

stabilization mechanism of CS may be explained by the formation of some complexes between CS and FTJ through noncovalent interactions.

For the samples containing the SSPS + PUL + CS mixture, the absolute value of the zeta potential of the system significantly increased compared to that of each individually added hydrocolloid. This enhancement is attributed to the increased electrostatic repulsion between the droplets. Additionally, as the concentration of mixed hydrocolloids increases, the absolute value of the zeta potential also increases. When 0.15% SSPS + 0.03% PUL + 0.15% CS was added, the zeta potential reached its maximum, resulting in greater stability at this concentration.

The size of the particulate matter in the juice plays a crucial role in its physical stability and can influence consumer preference. Generally, juices with smaller particles exhibit better stability due to slower sedimentation rates than those with larger particles (Zhu et al., 2020). The presence of difficult-to-dissolve substances, which differ in density from fruit juice, is the main reason for juice precipitation under the influence of gravity. By adjusting the particle size and increasing the viscosity of the liquid, the stability of the juice can be improved according to Stokes' law.

The particle size distribution (PSD) and size of the FTJ particles were influenced by different hydrocolloid treatments. Smaller particles impact D[3,2] (surface area-weighted mean diameter), while larger particles influence D[4,3] (volume-weighted mean diameter) (Yu et al., 2016). The values of D[3,2], D[4,3], D10, D50, and D90 for the FTJ subjected to different hydrocolloid treatments are presented in Table 1. The D[4,3] values of the control samples are nearly 2.6 times greater than the D[3,2] values, indicating a greater number of large particles than small particles (Leite et al., 2015). Upon adding 0.25% SSPS, the D[4,3], D[3,2], and D50 values decreased, suggesting that hydrocolloid treatments affect both large and small particles in the FTJ samples. Fig. 3 illustrates the impact of different hydrocolloids on the particle size distribution of the FTJ samples. The PSD of all FTJ samples is shown in Fig. 3, with peaks representing the different components of the FTJ.The addition of SSPS and CS shifted the peaks to the left, indicating an increase in the percentage of smaller particles, particularly when 0.25% SSPS was added. This could be attributed to the reactions that reduce the cellular structure of plant tissues within the FTJ (Ke et al., 2022). When PUL was added alone or in a mixture with other hydrocolloids, the mean particle sizes calculated by D[4,3] and D[3,2] were greater than those of samples without the addition of colloids, suggesting that they may stabilize the samples by altering viscosity rather than particle size. In conclusion, the stability of FTJ can be adjusted by modifying the average particle size and increasing the viscosity of the liquid.

Table 1
Particle size of the FTJ after different hydrocolloid treatments.

Strains	D[4,3] (μm)	D[3,2] (μm)	d10 (μm)	d50 (μm)	d90 (μm)
Blank	15.23 ± 1.42^{de}	5.76 ± 0.20^{e}	2.61 ± 0.11^{f}	8.64 ± 0.33^{f}	22.68 ± 0.98^{f}
0.15%SSPS	11.3 ± 0.63^{e}	4.71 ± 0.04^{f}	2.14 ± 0.02^{g}	6.58 ± 0.08^{h}	19.47 ± 0.62^{fg}
0.2%SSPS	12.37 ± 0.41^{e}	4.65 ± 0.13^{f}	2.10 ± 0.10^{g}	6.50 ± 0.09^{h}	20.45 ± 1.29^{fg}
0.25%SSPS	10.72 ± 1.59^{e}	4.13 ± 0.05^{a}	1.88 ± 0.01^{h}	5.52 ± 0.09^{i}	18.84 ± 1.42^{fg}
0.02%PUL	36.30 ± 1.02^{a}	15.97 ± 0.09^{g}	9.56 ± 0.08^{a}	28.50 ± 0.21^{b}	71.69 ± 1.36^{a}
0.04%PUL	29.43 ± 9.75^{ab}	8.76 ± 0.11^{c}	4.54 ± 0.04^{c}	14.74 ± 0.12^{d}	40.49 ± 4.51^{c}
0.06%PUL	15.48 ± 0.55^{de}	6.59 ± 0.11^{d}	2.91 ± 0.05^{d}	10.93 ± 0.24^{e}	27.46 ± 0.97^{e}
0.2%CS	11.45 ± 1.15^{e}	4.24 ± 0.01^{g}	1.95 ± 0.01^{h}	5.72 ± 0.03^{i}	18.90 ± 0.79^{g}
0.25%CS	11.07 ± 1.12^{e}	4.34 ± 0.16^{g}	2.01 ± 012^{h}	5.84 ± 0.15^{hi}	17.81 ± 1.13^{g}
0.3%CS	12.55 ± 1.17^{e}	4.20 ± 0.05^{g}	1.91 ± 0.01^{h}	5.66 ± 0.10^{i}	20.27 ± 0.93^{fg}
0.05%SSPS+0.01% PUL + 0.05%CS	22.92 ± 1.33^{bc}	9.69 ± 0.14^{b}	4.76 ± 0.09^{b}	17.62 ± 0.31^{c}	45.33 ± 2.13^{b}
0.1%SSPS+0.02% PUL + 0.1%CS	20.37 ± 4.58^{cd}	5.90 ± 0.09^{e}	2.44 ± 0.02^{e}	9.84 ± 0.19^{g}	29.34 ± 1.85^{e}
0.15%SSPS+0.03% PUL + 0.15%CS	20.33 ± 0.89^{cd}	5.71 ± 0.04^{e}	2.31 ± 0.01^{e}	9.62 ± 0.12^{g}	33.23 ± 0.28^{d}

Mean ± standard deviation; the significance of differences between groups was assessed based on the mean ($n = 3$) and calculated at a significance level of $P < 0.05$; different lowercase letters indicate significant differences.

3.2. Rheological characterization

The stability and sensory characteristics of juice drinks are significantly influenced by their rheological properties (Quintana-martinez et al., 2022). The rheological behavior of juice beverages is impacted by the properties of the continuous phase (such as viscosity, chemical composition, and polarity) and the dispersed phase (including particle size distribution, shape, surface properties, and interparticle interactions) (Zhu et al., 2020). All FTJ samples exhibited a notable decrease in apparent viscosity and a rapid increase in shear stress, displaying non-Newtonian pseudoplastic fluid behavior. This was attributed to the disruption of the network structure under the shear rate (Liu et al., 2019). As the shear rate increases, the molecular coordination gradually depolymerizes becauseto electrostatic interactions, resulting in shear thinning.

In line with Stokes' law, high viscosity impedes or delays the precipitation of particles, making viscosity a pivotal factor in stabilizing beverages through the use of polysaccharides. Additionally, the branching structure, chemical composition, and molecular weight of polysaccharides can impact viscosity (Lan et al., 2018). The viscosities of SSPS, PUL, and CS in the FTJ at different shear rates are depicted in Fig. 4A. Compared with the shear stress, the viscosity of the FTJ decreased with increasing shear rate. In the case of SSPS, an anionic polysaccharide, the viscosities remained nearly unchanged compared with those of the control group at 0.15% and 0.2% additions, while they increased at the 0.25% level. This could be attributed to the viscosity increase due to the increase in the suspended particle concentration with increasing addition. The viscosity of CS-treated FTJ was not notably affected compared to that of the control, resembling the behavior of gum arabic, where droplets are stabilized by electrostatic interactions, and the system viscosity is not significantly altered (Shao et al., 2020). The addition of PUL, a neutral polysaccharide, also increased the viscosity of the system, with a more pronounced effect than that observed after the addition of SSPS (Fig. 4A and Fig. 4B). This is likely because PUL, formed by the polymerization of maltotriose repeating units linked by α-1,4 glycosidic bonds via α-1,6 glycosidic bonds, possesses a greater viscosity, contributing to the overall viscosity of the beverage.

FTJ prepared with multiple hydrocolloids exhibited greater viscosity than those prepared with a single hydrocolloid at all shear rates. Furthermore, the viscosity of the compounded hydrocolloids gradually increased with increasing hydrocolloid additive quantity, reaching a maximum viscosity when the addition amount was 0.15% SSPS + 0.03% PUL + 0.15% CS. This behavior aligns with previous studies that demonstrated that synergistic viscosity increases with the combination of xanthan and guar gums and spiny bean gums (Saha & Bhattacharya, 2010). In this study, a certain range of stability and other rheological properties were more effectively stabilized with the addition of a mixture of SSPS, PUL, and CS than with the addition of a single hydrocolloid, which may be due to spatial and nonstationary repulsive, hydrophobic partial interactions induced through the simultaneous use of multiple hydrocolloids. This may also elucidate the improvement in stability when using a combination of multiple hydrocolloids.

3.3. FTIR analysis

FTIR spectroscopy was used to further characterize the structure of

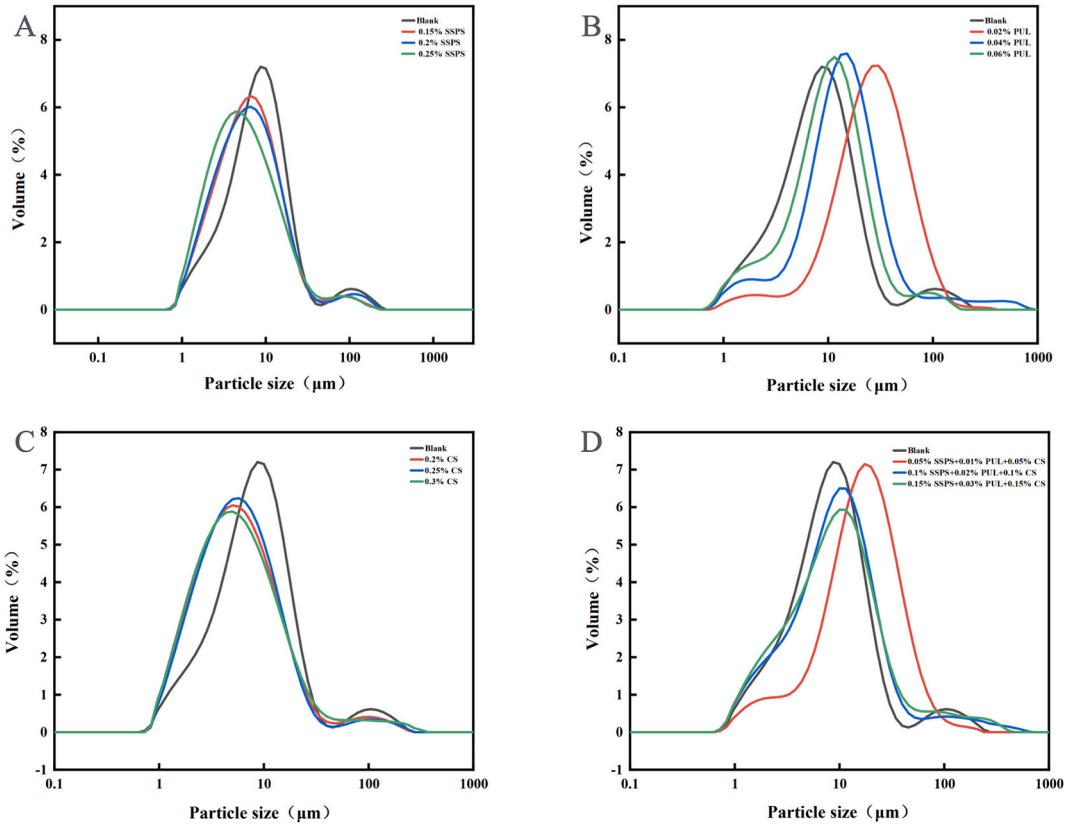

Fig. 3. Particle size distributions of FTJ with different hydrocolloid treatments.

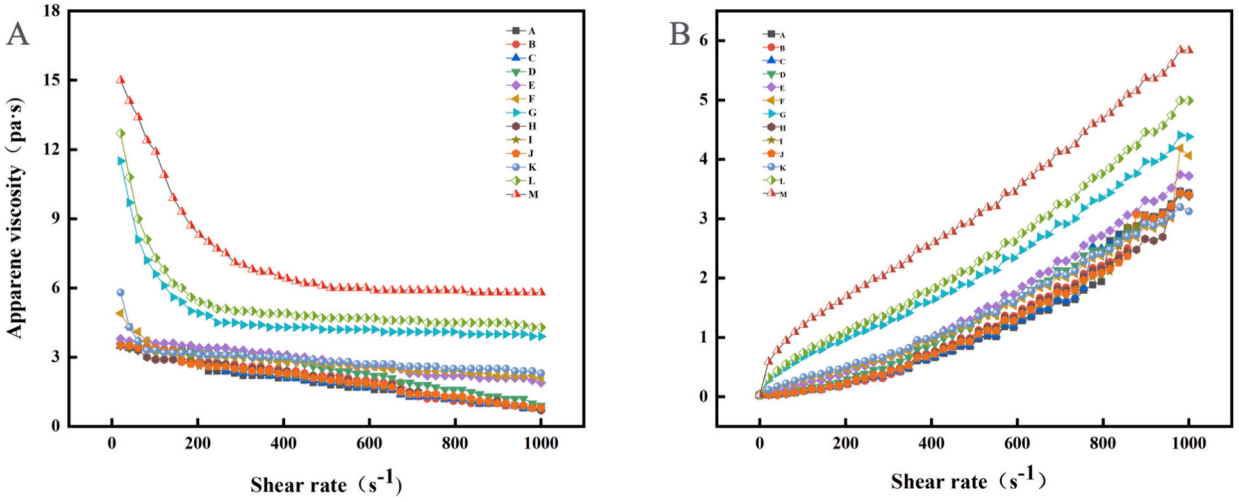

Fig. 4. A. Effect of the apparent viscosity of the FTJ after different hydrocolloid treatments. B. Effect of shear strength on the FTJ after different hydrocolloid treatments. A: Blank; B: 0.15%SSPS; C: 0.2%SSPS; D: 0.25%SSPS; E: 0.02%PUL; F: 0.04%PUL; G: 0.06%PUL; H: 0.2%CS; I: 0.25%CS; J: 0.3%CS; K: 0.05% SSPS+0.01%PUL + 0.05%CS; L: 0.1%SSPS+0.02%PUL + 0.1%CS; M: 0.15%SSPS+0.03%PUL + 0.15%CS.

the FTJ samples from the control and experimental groups, as illustrated in Fig. 5. All the samples displayed the typical FTIR characteristics of tomatoes: C—H stretching vibrations in the 3000–2800 cm^{-1} range due to carbohydrates, proteins, and organic acids in the FTJ and peaks in the 3200–3550 cm^{-1} and 1300–1000 cm^{-1} ranges attributed to the IR absorption peaks of O—H in water and carbohydrates in the FTJ (Tao et al., 2021). The absorption peaks in the 1680–1630 cm^{-1} range were caused by the IR absorption of amide bonds in the proteins in the FTJ, while those in the 1450–1300 cm^{-1} range were due to the stretching vibration of the -COO of some volatile organic acids in the FTJ (Wang et al., 2023).

Fig. 5 shows that the absorption peak of -OH in the 3550–3200 cm^{-1} range shifted after the addition of SSPS, PUL, and CS to the FTJ. These absorption peaks were all shifted toward higher frequencies than those of the FTJ without the addition of hydrocolloids. This observation suggested that some proteins or carbohydrates in FTJ may bind to polysaccharides and form hydrogen-bonding interactions with hydrocolloids. Additionally, the absorption peaks in the 1680–1630 cm^{-1} range were shifted toward higher frequencies than those of FTJ without hydrocolloid addition, possibly due to structural changes in the amide bonds in the protein affected by the addition of hydrocolloid.

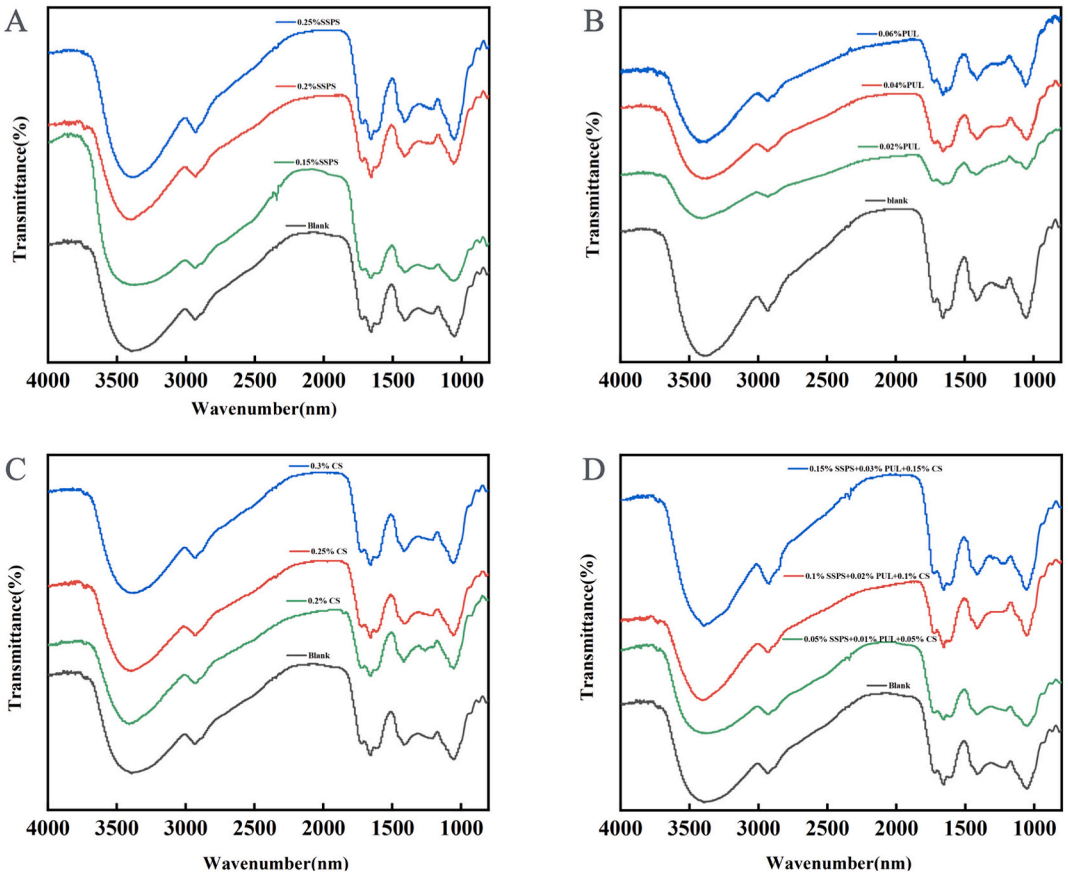

Fig. 5. FTIR spectra of FTJ with different hydrocolloid treatments.

Furthermore, the intensity of the absorption peak of -OH in the 3550–3200 cm^{-1} range gradually increased with increasing hydrocolloid concentration. This was because the hydrocolloids are composed of monosaccharides with polyhydroxy aldehydes or polyhydroxy ketones linked by glycosidic bonds, and the introduction of hydrocolloids results in an increase in the number of hydroxyl groups in the sample. Overall, the addition of hydrocolloids may facilitate the combination of polysaccharides with proteins and carbohydrates in tomatoes through hydrogen bonding (Paola et al., 2024).

3.4. Surface tension analysis

Surface tension is the ability of liquid molecules to attract each other, maintaining the stability and elasticity of the liquid surface. A higher surface tension indicates greater resistance to flow and improved stability. The changes in surface tension over time for different samples are depicted in Fig. 6. The surface tension values reflected the surface activity of the samples. With the addition of 0.02% PUL, the surface tension at stabilization was 40.5 mN/m, which was greater than that with the addition of PUL and CS. This could be attributed to the significant influence of the produced PUL structure, indicating the crucial role of hydrophilic and hydrophobic functional groups. When the three hydrocolloids were combined, the surface tension with the addition of 0.15% SSPS + 0.03% PUL + 0.15 CS reached 42.6 mN/m, demonstrating substantial surface activity. This suggested that the presence of hydrophobic compounds contributed to the overall amphiphilicity of the macromolecules (Nikola et al., 2023).

3.5. Stability analysis

To further understand the impact of the polysaccharides SSPS, PUL, and CS on the physical stability of the FTJ, a LUMiSizer dispersion analyzer was used to track the evolution of the transport curves of SSPS, PUL, and CS, as depicted in Fig. 7. The experimental setup gradually separates the FTJ through centrifugation, with the transport curves of the FTJ recorded from the initial to the final stages (Wu et al., 2020). The

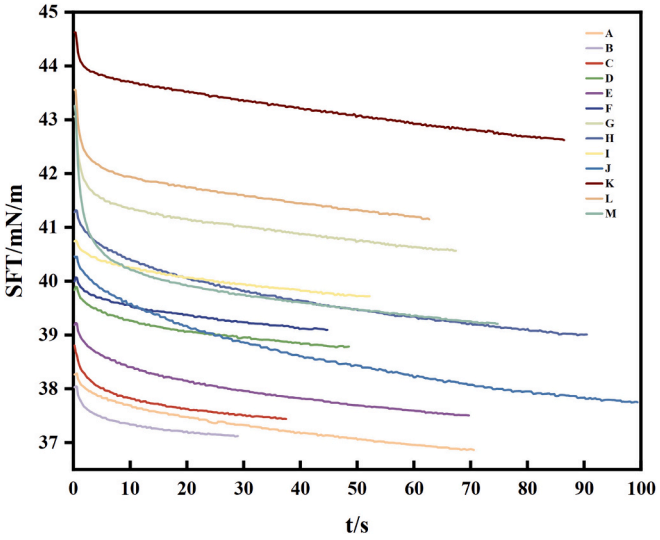

Fig. 6. Surface tension of the FTJ after different hydrocolloid treatments. A: Blank; B: 0.15%SSPS; C: 0.2%SSPS; D: 0.25%SSPS; E: 0.02%PUL; F: 0.04%PUL; G: 0.06%PUL; H: 0.2%CS; I: 0.25%CS; J: 0.3%CS; K: 0.05%SSPS+0.01%PUL + 0.05%CS; L: 0.1%SSPS+0.02%PUL + 0.1%CS; M: 0.15%SSPS+0.03%PUL + 0.15%CS.

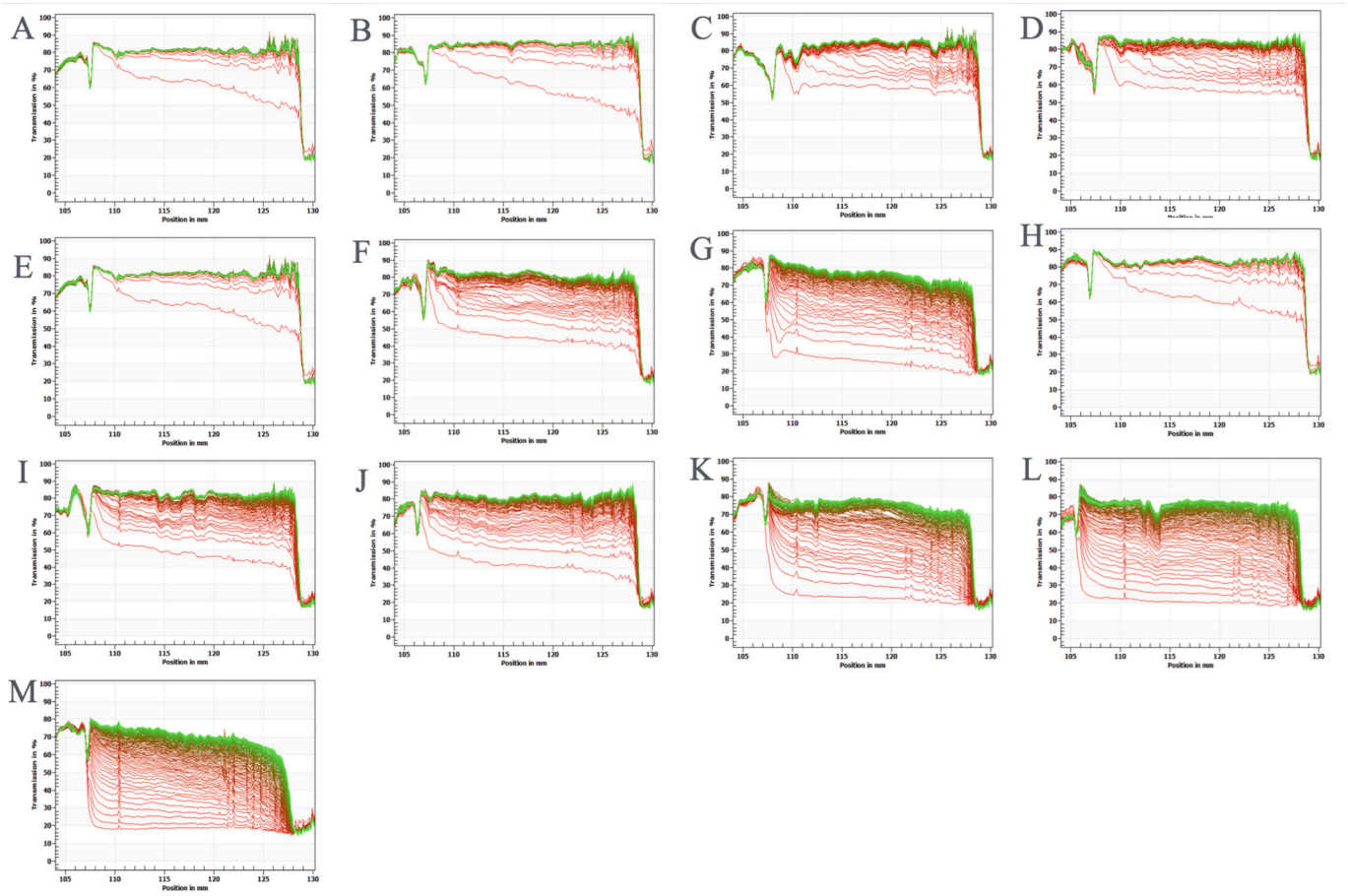

Fig. 7. Evolution of transmission curves for FTJ with different hydrocolloid treatments. A: Blank; B: 0.15%SSPS; C: 0.2%SSPS; D: 0.25%SSPS; E: 0.02%PUL; F: 0.04% PUL; G: 0.06%PUL; H: 0.2%CS; I: 0.25%CS; J: 0.3%CS; K: 0.05%SSPS+0.01%PUL + 0.05%CS; L: 0.1%SSPS+0.02%PUL + 0.1%CS; M: 0.15%SSPS+0.03%PUL + 0.15%CS.

first transmission profile is represented by the red line at the bottom, while the last transmission profile is indicated by the green line at the top. This profile illustrates the changes in sample transmittance at various positions and over extended settling times. Initially, all FTJ systems were uniformly dispersed and opaque, but as centrifugation progressed, they began to destabilize and gradually precipitated at the bottom of the sample tube. Consequently, the transport at the bottom of the sample tube increased, and the newly recorded red profiles gradually moved toward the top until the last green profile was recorded. A higher migration rate indicated greater destabilization. Throughout centrifugation, all samples exhibited significant changes in nonoverlapping transmission spectra and transmission values, signifying phase

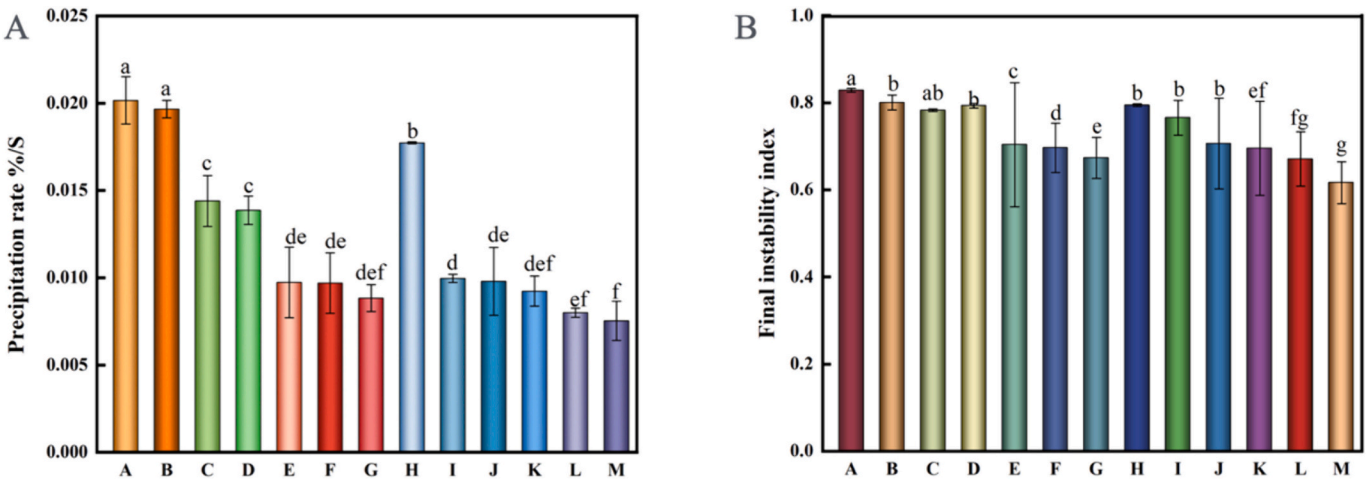

Fig. 8. A. Precipitation rates of FTJ with different hydrocolloid treatments. B Final instability coefficients of FTJ with different hydrocolloid treatments. A: Blank; B: 0.15%SSPS; C: 0.2%SSPS; D: 0.25%SSPS; E: 0.02%PUL; F: 0.04%PUL; G: 0.06%PUL; H: 0.2%CS; I: 0.25%CS; J: 0.3%CS; K: 0.05%SSPS+0.01%PUL + 0.05%CS; L: 0.1%SSPS+0.02%PUL + 0.1%CS; M: 0.15%SSPS+0.03%PUL + 0.15%CS.

separation and precipitation. The stability of the sample was reflected in the compactness and smoothness of the plot lines (Niu et al., 2022), with the best stability observed with the addition of 0.15% SSPS + 0.03% PUL + 0.15% CS.

As depicted in Fig. 8A, we analyzed the sedimentation rates of FTJ with different hydrogel treatments to visually compare the changes in transport. For the SSPS, PUL, and CS treatments, the overall transfer rate of the samples gradually decreased with increasing concentration, indicating slower sedimentation rates and enhanced stability. The most effective stabilization was achieved with the combination of 0.15% SSPS, 0.03% PUL, and 0.15% CS, resulting in a sedimentation rate of 0.0065.

The variations in the FTJ instability index and final instability index over time for the SSPS, PUL, and CS treatments are presented in Fig. 8B and Fig. 9. The instability index represents the ratio of the clarification obtained by the sample at a fixed separation time to the maximum clarification (Fernandes et al., 2017). This value ranges between 0 and 1, with 0 indicating no change and high stability and 1 indicating complete dispersion separation and high instability. Initially, all the FTJ were uniformly distributed and stable, without stratification. However, as centrifugation time increased, the FTJ gradually began to separate, leading to larger degrees of clarification and increased instability indices. With increasing SSPS concentration, the instability index initially decreased and then increased, reaching its minimum at 0.25%, indicating the highest stability at this concentration. Compared with the FTJ stabilized by 0.2% SSPS, the FTJ stabilized by 0.25% SSPS exhibited a lower particulate content, higher viscosity, and a thicker interfacial layer. However, the 0.25% SSPS-stabilized FTJ displayed poorer stability, possibly due to the inferior elasticity of the interfacial layer, resulting in a reduced stabilization effect. In contrast, PUL and CS showed a gradual decrease in the instability index with increasing concentration, suggesting that the instability coefficients of the FTJ stabilized by PUL and CS were directly proportional to the concentration, leading to enhanced stability. Similar results were observed in a previous study, where higher xanthan gum concentrations in water resulted in stronger sample stabilization (Kuentz, & Röthlisberger, D., 2003). Overall, when a single hydrocolloid was used, the stabilizing effect of PUL surpassed that of both SSPS and CS. Compared to SSPS, CS, and PUL alone, the three hydrocolloid complexes demonstrated clear advantages over FTJ in terms of long-term stability, likely due to their higher viscosity and surface tension. This can be attributed to the synergistic effect of the cocolloids and their strong water-absorption capacity (Abedi et al., 2014).

While LUMiSizer currently shows promise as an alternative for long-term stability studies, additional measurements of beverages should be performed to confirm the potential use of LUMiSizer for accelerating and replacing storage.

4. Conclusion

In this study, the impact of three hydrocolloids with different charges (SSPS, PUL, and CS) on the stability of FTJ was investigated. The

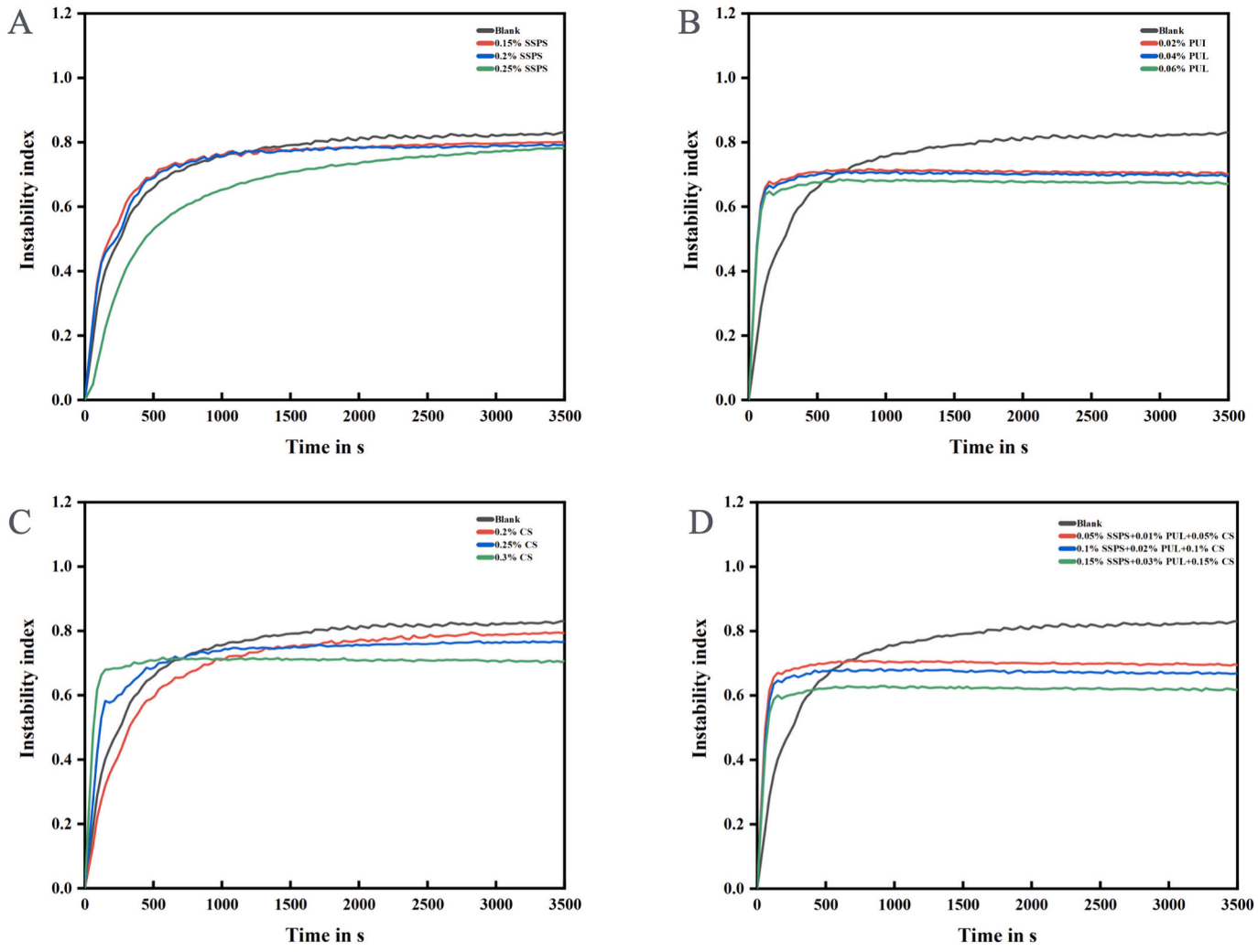

Fig. 9. Instability coefficients of FTJ with different hydrocolloid treatments.

analysis included particle size, zeta potential, rheological properties, Fourier transform infrared spectroscopy, surface tension, instability coefficient, and sedimentation rate. Compared with the other two polysaccharides, the addition of PUL significantly improved the stability of FTJ, possibly because of the unique structure of PUL. The most effective stabilization was achieved with a polysaccharide ratio of 0.15% SSPS + 0.03% PUL + 0.15% CS, resulting in lower instability coefficients, lower sedimentation rates, and higher viscosity and zeta potential. These findings indicate the crucial role of the instability coefficient, sedimentation rate, viscosity, and zeta potential in the stability of FTJ. This study provides a comprehensive analysis of the effects of these three hydrocolloids on FTJ stability, offering promising prospects for their application in the beverage industry.

Funding

This work was supported by research on key technologies for the deep processing of Xinjiang's characteristic byproducts and the subtheme "Comprehensive Utilization of Tomato Processing Byproducts" of the Key Research and Development Special Project of the Autonomous Region (Xinjiang Uygur Autonomous Region, China) (2022B02004–3).

CRediT authorship contribution statement

Lei Zhao: Writing – review & editing, Writing – original draft. **Yu Wang:** Writing – review & editing. **Ruxianguli Maimaitiyiming:** Supervision. **Runhan Liu:** Visualization. **Liang Wang:** Writing – review & editing, Funding acquisition. **Ruoqing Liu:** Methodology. **Keping Chen:** Funding acquisition. **Aihemaitijiang Aihaiti:** Writing – review & editing, Funding acquisition. **Jingyang Hong:** Writing – review & editing.

Declaration of competing interest

The authors declare no conflicts of interest.

Data availability

Data will be made available on request.

Acknowledgments

The authors are also indebted to the anonymous reviewers for their constructive comments and suggestions for improving this manuscript.

References

Abedi, F., Sani, A. M., & Karazhiyan, H. (2014). Effect of some hydrocolloids blend on viscosity and sensory properties of raspberry juice-milk. *Journal of Food Science & Technology, 51*, 2246–2250.

Dai, T. T., Li, R. Y., Liu, C. M., Liu, W., Li, T., Chen, J., … David, J. M. (2019). Effect of riceglutelin-resveratrol interactions on the formation and stability of emulsions: Amultiphotonic spectroscopy and molecular docking study. *Food Hydrocolloids, 105234*.

Dammak, I., Sobral, P., & J.A.. (2018). Effect of different biopolymers on the stability of hesperidin encapsulating O/W emulsions. *Journal of Food Engineering, 237*, 33–43.

Fernandes, A., Ferreira, N., Fangueiro, J., Santos, A., Veiga, F., Cabral, C., & Silva, & A., Souto, E.. (2017). Ibuprofen nanocrystals developed by 22 factorial design experiment: A new approach for poorly water-soluble drugs. *Saudi Pharmaceutical Journal, 25*, 1117–1124.

Fredrik, I., Maytham, A., Ulrich, H. K., & Andreas, H. A. (2020). Mechanistic investigation of cell breakup in tomato juice homogenization. *Journal of Food Engineering, 272*, Article 109858.

Giovanelli, G., & Paradiso, A. (2022). Stability of dried and intermediate moisture tomato pulp during storage. *Journal of Agricultural and Food Chemistry, 50*, 7277–7281.

Hartgerink, J. D., Beniash, E., & Stupp, S. I. (2001). Self-assembly and mineralization of peptide-amphiphile nanofibers. *Science, 294*, 1684–1688.

Huang, K., Zhang, S., Guan, X., Li, C., Li, S., Liu, Y., & Shi, J. (2021). Effect of the oat β-glucan on the development of functional quinoa (Chenopodium quinoa wild) milk. *Food Chemistry, 349*, Article 129201.

Ke, Y. Y., Dai, T. T., Xiao, M., Chen, M. S., Liang, R. H., Liu, W., … Deng, L. Z. (2022). Industry-scale microfluidizer system produced whole mango juice: Effect on the physical properties, microstructure and pectin properties innovative. *Food Science and Emerging Technologies, 75*, Article 102887.

Kuentz, M., & Rothlisberger, D.. (2003). Rapid assessment of sedimentation stability in dispersions using near-infrared transmission measurements during centrifugation and oscillatory rheology. *European Journal of Pharmaceutics and Biopharmaceutics, 56*, 355–361.

Lan, Y., Chen, B., & Rao, J. (2018). Pea protein isolates-high methoxyl pectin soluble complexes for improving pea protein functionality: Effect of pH, biopolymer ratio and concentrations. *Food Hydrocolloids, 80*, 245–253.

Leite, T. S., Augusto, P. E., & Cristianini, M. (2015). Using high-pressure homogenization (HPH) to change the physical properties of cashew apple juice. *Food Biophysics, 10*, 169–180.

Lisa, S., Agnes, M. R., El, M. R., Gertrude, B., Lisa, S., Marion, W., … Marc, P. (2023). Combinations of hydrocolloids show enhanced stabilizing effects on cloudy orange juice ready-to-drink beverages. *Food Hydrocolloids, 138*, Article 108436.

Liu, S., Sun, C., Xue, Y., & Gao, Y. (2016). Impact of pH, freeze-thaw, and thermal sterilization on physicochemical stability of walnut beverage emulsion. *Food Chemistry, 196*, 475–485.

Liu, Z., Bhandari, B., Prakash, S., Mantihal, S., & Zhang, M. (2019). Linking rheology and printability of a multicomponent gel system of carrageenan-xanthan-starch in extrusion-based additive manufacturing. *Food Hydrocolloids, 87*, 413–424.

Nakamura, A., Yoshida, R., Maeda, H., & Corredig, M. (2006). The stabilizing behavior of soybean soluble polysaccharide and pectin in acidified milk beverages. *International Dairy Journal, 16*, 361–369.

Nikola, M., Zita, S., Veljko, K., Petar, D., Nemanja, T., & Ljubica, D. (2023). Comparative characterization of sugar beet fibers to sugar beet pectin and octenyl succinic anhydride modified maltodextrin in aqueous solutions using viscometry, conductometry, tensiometry, and component analysis. *Journal of the Science of Food and Agriculture, 103*, 255–263.

Niu, H., Chen, X. W., Luo, T., Chen, H. M., & Fu, X. (2022). The interfacial behavior and long-term stability of emulsions stabilized by gum arabic and sugar beet pectin. *Carbohydrate Polymers, 291*, Article 119623.

No, H., & Prinyawiwatkul, W. (2009). Stability of chitosan powder during long-term storage at room temperature. *Journal of Agricultural and Food Chemistry, 57*, 8434–8438.

Okuyama, K., Noguchi, K., Kanenari, M., Egawa, T., & Ogawa, K. (2000). Structual diversity of chitosan and its complexs. *Carbohydrate Polymer, 41*, 237–247.

Paola, M. R., Beatriz, M. L., Francisco, J. B. B., Pedro, U. B. R., Nancy, D. R. H., Karla, M. R., & Ramsés, R. G. E. (2024). Active films and coatings based on commercial chitosan with natural extracts addition from coconut by-products: Physicochemical characterization and antifungal protection on tomato fruits extracts addition from coconut by-products: Physicochemical characterization and antifungal protection on tomato fruits. *Food Control, 155*, Article 110077.

Pedro, E. D. A., Albert, I., & Marcelo, C. (2013). Effect of high-pressure homogenization (HPH) on the rheological properties of tomato juice: Creep and recovery behaviours. *Food Research International, 54*, 169–176.

Quintana-martinez, S. E., Torregroza-fuentes, E. E., & García-zapateiro, L. A. (2022). Rheological and microstructural properties of acidified Milk drink stabilized with butternut squash pulp hydrocolloids (BSPHs). *ACS Omega, 7*, 19235–19242.

Ram, S. S., Navpreet, K., Dhandeep, S., & John, F. (2019). Kennedy investigating aqueous phase separation of pullulan from Aureobasidium pullulans and its characterization. *Carbohydrate Polymers, 223*, Article 115103.

Ruly, T. H., Joana, G. S., Nicole, B. S., Muhammad, A., Silvio, S. S., & Júlio, C. S. (2019). Low-pressure homogenization of tomato juice using hydrodynamic cavitation technology: Effects on physical properties and stability of bioactive compounds. *Ultrasonics-Sonochemistry, 54*, 192–197.

Saha, D., & Bhattacharya, S. (2010). Hydrocolloids as thickening and gelling agents in food: A critical review. *Journal of Food Science and Technology, 47*, 587–597.

Shao, P., Feng, J., Sun, P., Xiang, N., Lu, B., & Qiu, D. (2020). Recent advances in improving stability of food emulsion by plant polysaccharides. *Food Research International, 137*, Article 109376.

Sinchaipanit, P., Kerr, W. L., & Chamchan, R. (2013). Effect of sweeteners and hydrocolloids on quality attributes of reduced-calorie carrot juice. *Journal of the Science of Food and Agriculture, 93*, 3304–3311.

Souza, F. N., Gebara, C., Ribeiro, M. C. E., Chaves, K. S., Gigante, M. L., & Grosso, C. R. F. (2012). Production and characterization of microparticles containing pectin and whey proteins. *Food Research International, 49*, 560–566.

Tao, Z., Zhiming, W., Shujuan, Y., Xiaoming, G., Chao, A., Xiangyi, T., Hualei, C., Jiawei, L., Xuan, Z., & Hecheng, M. (2021). Effects of pH and temperature on the structure, rheological, and gel-forming properties of sugar beet pectins. *Food Hydrocolloids, 116*, Article 106646.

Tiwari, B. K., Muthukumarappan, K., Donnell, C. P. O., & Cullen, P. J. (2009). Inactivation kinetics of pectin methylesterase and cloud retention in sonicated orange juice. *Innovative Food Science & Emerging Technologies, 10*, 166–171.

Wang, Y. R., Yang, Q., Du, Y. N., & Chen, H. Q. (2023). Chitosan can improve the storage stability of ovalbumin fibrils at pH higher than isoelectric point. *Food Hydrocolloids, 136*, Article 108286.

Wei, Y., Cai, Z., Wu, M., Guo, Y., Tao, R., Li, R., Wang, P., Ma, A., & Zhang, H. (2020). Comparative studies on the stabilization of pea protein dispersions by 837 using various polysaccharides. *Food Hydrocolloids, 98*(105233), 838.

Wu, W. Y., Li, L., Hong, Z. H., & Xie, X. N. (2020). Comparison of emulsifying characteristics of different macromolecule emulsifiers and their effects on the physical properties of lycopene nanoemulsions. *Journal of Dispersion Science and Technology, 41*, 618–627.

Xiao, Q., Lim, L., Zhou, Y., & Zhao, Z. (2017). Drying process of pullulan edible films forming solutions studied by lowfield NMR. *Food Chemistry, 230*, 611–617.

Yoo, S. H., Fishman, M. L., Hotchkiss, A. T., & Lee, H. G. (2006). Viscometric behavior of high-methoxy and low-methoxy pectin solutions. *Food Hydrocolloids, 20*, 62–67.
Yu, Z. Y., Jiang, S. W., Cao, X. M., Jiang, S. T., & Pan, L. J. (2016). Effect of high-pressure homogenization (HPH) on the physical properties of taro (Colocasia esculenta (L). Schott) pulp. *Journal of Food Engineering, 177*, 1–8.
Zhang, Z., Yang, Y., Huang, X., Jin, Z., & Jiao, A. (2023). Stabilization of a collagen peptide-cranberry juice by three functional polysaccharides with different charge characteristics. *Food Hydrocolloids, 139*, Article 108518.
Zhao, L., Maimaitiyiming, R., Hong, J, Y., Wang, L., Mu, Y., Liu, B, Z., Zhang, H, M., Chen, K, P., & Aihait, A. (2024). Optimization of tomato (Solanum lycopersicum L.) juice fermentation process and analysis of its metabolites during fermentation. Frontiers in Nutrition, 1344117.
Zhu, D. S., Shen, Y. S., Wei, L. W., Xu, L. X., Cao, X. H., Liu, H., & Li, J. R. (2020). Effect of particle size on the stability and flavor of cloudy apple juice. *Food Chemistry, 328*, 26967.